

Theory of Rheology and Aging of Protein Condensates

Ryota Takaki¹, Louise Jawerth², Marko Popović^{1,3,4,*} and Frank Jülicher^{1,3,4,†}

¹Max Planck Institute for the Physics of Complex Systems, Nöthnitzer Str. 38, 01187 Dresden, Germany

²Soft Matter Physics, Huygens-Kamerlingh Onnes Laboratory, Leiden University, P.O. Box 9504, 2300 RA Leiden, The Netherlands

³Cluster of Excellence Physics of Life, TU Dresden, 01062 Dresden, Germany

⁴Center for Systems Biology Dresden, 01307 Dresden, Germany



(Received 31 March 2023; accepted 21 July 2023; published 4 August 2023)

Biological condensates are assemblies of proteins and nucleic acids that form membraneless compartments in cells and play essential roles in cellular functions. In many cases they exhibit the physical properties of liquid droplets that coexist in a surrounding fluid. Recently, quantitative studies on the material properties of biological condensates have become available, revealing complex material properties. *In vitro* experiments have shown that protein condensates exhibit time dependent material properties, similar to aging in glasses. To understand this phenomenon from a theoretical perspective, we develop a rheological model based on the physical picture of protein diffusion and stochastic binding inside condensates. The complex nature of protein interactions is captured by a distribution of binding energies, incorporated in a trap model originally developed to study glass transitions. Our model can describe diffusion of constituent particles, as well as the material response to time-dependent forces, and it recapitulates the age dependent relaxation time of Maxwell glass observed experimentally both in active and passive rheology. We derive fluctuation-response relations of our model in which the relaxation function does not obey time translation invariance. Our study sheds light on the complex material properties of biological condensates and provides a theoretical framework for understanding their aging behavior.

DOI: [10.1103/PRXLife.1.013006](https://doi.org/10.1103/PRXLife.1.013006)

I. INTRODUCTION

The formation of biological condensates by phase separation of proteins and nucleic acids in the cell has become a new paradigm in molecular biology over the last decade [1–3]. Such condensates provide membraneless biochemical compartments with liquidlike properties. They typically exhibit a spherical shape to minimize the surface tension and have properties of droplets in a fluid environment. Recent studies suggest that rheological properties of biomolecular condensates can be considerably richer than those of simple liquids [4–6], which may have biological consequences [6–9].

Recently, the rheological property of RNA associated condensates of PGL-3 and FUS protein condensates were studied *in vitro* using active and passive microrheology [5]. The study revealed time-dependent material properties of these protein condensates, summarized as follows: (1) The rheological properties of the condensates depend on the waiting time (t_w) between droplet formation and experiment; they are well fit by a Maxwell fluid model with elastic behavior on short time scales up to the relaxation time (τ_c) and liquid behavior at the longer time scales. (2) The relaxation time, τ_c , of the

Maxwell fluid increases for longer waiting time t_w . The increase of τ_c is associated with a strong increase of viscosity, while the change of elasticity is small. (3) Various quantities reflecting the material property, such as complex modulus and mean-squared displacement, collapse on a master curve upon rescaling of frequency and modulus for different t_w . These time-dependent rheological properties suggest that the rheology of the protein condensates is an aging Maxwell fluid, termed Maxwell glass, referring to aging phenomena in glassy materials [10,11].

Viscoelastic properties of condensates have been reported in multiple experimental studies. Alshareedah *et al.* [12] found that condensate viscoelasticity can be modulated by varying aminoacid sequence of condensate-forming proteins. Ghosh *et al.* [4] investigated the relationship between condensate rheology and fusion dynamics showing that shorter relaxation times lead to faster fusion. Theory on viscoelastic condensates has addressed the shape dynamics of condensate droplets [13], as well as salt dependence of viscoelastic material properties [14]. A two fluid model describing the transition from a liquid to an elastic droplet was proposed to discuss the observed solidlike condensate behaviors [15]. Shen *et al.* [16] reported the spatially heterogeneous condensate organization during the transition from a liquid to a solid state in an aging condensate.

Aging and complex rheology of nonbiological materials has a long history of research [17] due to its abundance and close connection to daily life [18]. A comprehensive experimental study of aging materials by Struik dates back to the 1970s [19]. More recently, aging colloidal glasses have been studied using microrheology [20]. The soft glassy rheology

*Corresponding author: mpopovic@pks.mpg.de

†Corresponding author: julicher@pks.mpg.de

Published by the American Physical Society under the terms of the [Creative Commons Attribution 4.0 International](https://creativecommons.org/licenses/by/4.0/) license. Further distribution of this work must maintain attribution to the author(s) and the published article's title, journal citation, and DOI.

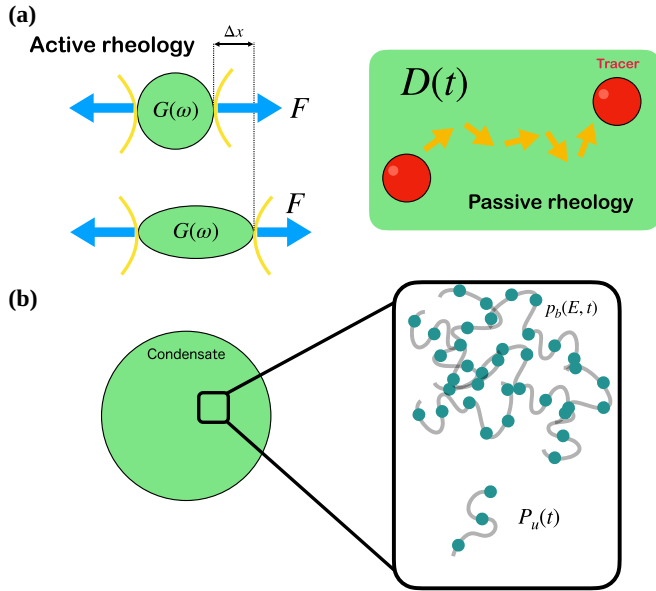


FIG. 1. Schematics of the model and methods of microrheology. (a) Left: Schematics of active rheology. The external force (F) is applied to the protein condensates (green spheres) having complex modulus $G(\omega)$ using optical tweezers (yellow). The relation between strain and stress gives the material property of condensates. Right: Schematics of passive rheology. The motion of the tracer element (red) embedded into the condensate is tracked. The element's mean square displacement encodes the condensate's material property, which manifests as diffusion coefficient $D(t)$. (b) Schematics of the model. The diffusing element takes two states. One is the bound state, where chemical crosslinks are densely connected at the reaction sites (green circles) so that the diffusion of the elements is hindered. The other is the unbound state, where the diffusing elements can freely undergo diffusive motion. We denote the probability density of the bound state as $p_b(E, t)$ and the probability of the unbound state as $P_u(t)$ (see the main text for the detail).

(SGR) model has been developed to describe the aging and rheology of soft materials [21–23], based on seminal works by Bouchaud and coworkers [24,25]. However, in the aging regime, the SGR model exhibits a solid-like behavior which does not describe an aging Maxwell fluid. Recently, Lin [26] proposed a related mean-field model for condensate aging, based on the assumption of strongly correlated transitions between trap energies, in contrast to the soft glassy rheology model. Calculating the linear response function in this model yields a linear aging of the condensate relaxation time scale.

In this work, we develop a mean-field model of aging biological condensates that can describe their time-dependent material properties, observed in experiments. We clarify how the aging of the protein condensates is reflected in active and passive microrheology. Active and passive rheology methods are illustrated in Fig. 1(a). The structure of the paper is as follows. In Sec. II, we propose a mean-field model to describe the binding and unbinding of diffusive elements inside the protein condensates. Using the unbound probability of elements in condensates, we write the constitutive equation of the aging Maxwell fluid, leading to the relaxation function for Maxwell glass (Sec. III A). In Sec. III C, we examine the time-dependent rheology of the model using active rheology

and propose the time-dependent complex modulus. Finally, in Sec. IV, we derive fluctuation-response relations between response functions and mean-squared displacement of the diffusive elements, which can be employed in passive rheology experiments. We conclude with a discussion of our results. For readers unfamiliar with the subject, we have included an introduction to the rheology of aging materials in Appendix A, which summarizes the essential concepts employed throughout the paper.

II. TRAP MODEL OF CONDENSATE AGING

We introduce a mean-field model of an aging protein condensate composed of crosslinked elements forming an elastic network. These elements occasionally unbind and freely diffuse before attaching at a new location, see Fig. 1(b). Dynamics of unbinding is determined by the binding energy E of individual crosslinks. To describe crosslinking of large proteins in a complex environment we draw binding energies from a distribution $\rho(E)$. The state of each crosslinker at time t is described by probabilities $p_b(E, t)$ and $P_u(t)$ to find it bound with energy E or unbound, respectively. In our mean-field model individual crosslinker probabilities also represent the fraction of all crosslinkers in the corresponding state. The dynamical equations for these probabilities are

$$\frac{1}{\Gamma_0} \frac{\partial p_b(E, t)}{\partial t} = -p_b(E, t)e^{-\beta E} + P_u(t)\rho(E), \quad (1a)$$

$$\frac{1}{\Gamma_0} \frac{\partial P_u(t)}{\partial t} = -P_u(t) + \int_0^\infty dE p_b(E, t)e^{-\beta E}, \quad (1b)$$

where $\beta \equiv 1/k_B T$, with temperature T and Boltzmann constant k_B . T is the temperature of the heat bath to which the condensates are coupled.

Equation (1) is an extension of trap model by Bouchaud [24,25]. The first term of the right-hand side in Eq. (1a) describes the transition from a bound state with energy $-E$ to the unbound state at $E = 0$, which occur at a rate $\Gamma_0 e^{-\beta E}$, where Γ_0 is a rate parameter and binding energy $E > 0$ is positive. The second term describes transitions from the unbound state to a bound state which occur at a density $\rho(E)$.

Here, we choose an exponential distribution of binding energies, $\rho(E) = \beta_0 e^{-\beta_0 E}$, which can describe both equilibrium and aging regimes of the model [24]. The parameter, $\alpha \equiv \beta_0/\beta$ controls qualitatively different solutions of Eq. (1). For $\alpha > 1$, the rate at which bound states are populated decays faster with E than the unbinding rate, and the system relaxes to an equilibrium steady state with $p_b^{\text{eq}}(E) \sim \rho(E) \exp(\beta E)$, and

$$P_u^{\text{eq}} = \frac{\alpha - 1}{2\alpha - 1}, \quad (2)$$

see Appendix C. As shown in Ref. [24], for $0 < \alpha < 1$ the rate at which bound state are populated decays slower with E than the unbinding rate, so that $p_b^{\text{eq}}(E)$ is no longer normalizable and the equilibrium state of Eq. (1) does not exist. The probability $P_u(t)$ vanishes asymptotically as

$$P_u(t) \simeq \kappa (\Gamma_0 t)^{\alpha-1}; \quad \kappa = \frac{1}{\alpha} \frac{\sin(\alpha\pi)}{\pi \Gamma[\alpha]}, \quad (3)$$

as derived in Appendix C. Here $\Gamma[\alpha]$ denotes the Gamma function. Figure 2 shows $P_u(t)$ for initial condition $P_u(t=0)$

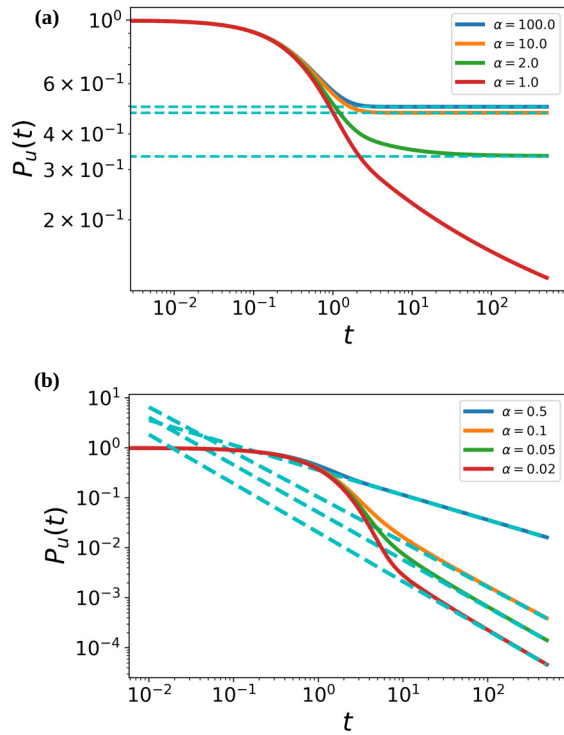


FIG. 2. Dynamics of the unbound probability $P_u(t)$. Solid lines are numerically obtained from Eq. (1) and dashed lines are analytical solutions from Eq. (2) or Eq. (3). The initial condition $p_b(E, 0) = 0$ ($P_u(t=0) = 1$). We set $\Gamma_0 = 1$, which characterizes the time scale of the initial relaxation ($t \approx 1/\Gamma_0$), and measure the time (t) in the unit of $1/\Gamma_0$. We fix β_0 to 1 and vary β . (a) $P_u(t)$ for $\alpha \geq 1$. The dashed lines in cyan are the analytical solutions from Eq. (2). The equilibrium solutions exist for $\alpha > 1$. (b) $P_u(t)$ for $\alpha < 1$. $P_u(t)$ shows aging dynamics (slow relaxation) for long time regime. The dashed lines in cyan are the analytical solutions from Eq. (3).

$= 1$ evaluated for different values of α , showing the equilibrium and aging dynamics.

To complete the model of an aging protein condensate we derive a mean-field constitutive equation of the condensate rheology. Crosslinked elements in the condensate are elastic with a shear modulus G_0 . When they unbind they can flow with viscosity η_0 . Crosslink binding and unbinding is accounted for by the trap model in Eqs. (1). The shear strain rate of an unbound element is $\dot{\epsilon}_u(t) = \sigma(t)/\eta_0$ while the strain of an element in the bound state is $\epsilon_b(t) = \sigma(t)/G_0$, where $\sigma(t)$ is the shear stress. Assuming the shear stress to be uniform within the condensate, the overall shear strain rate $\dot{\epsilon}(t) = P_u(t)\dot{\epsilon}_u(t) + (1 - P_u(t))\dot{\epsilon}_b(t)$ is therefore

$$\dot{\epsilon}(t) = \frac{\sigma(t)}{\eta_0} P_u(t) + \frac{\dot{\sigma}(t)}{G_0} (1 - P_u(t)). \quad (4)$$

This is an equation of a viscoelastic Maxwell material with an effective viscosity $\eta_c = \eta_0/P_u(t)$ and an effective elastic modulus $G_c = G_0/(1 - P_u(t))$, that can exhibit aging dynamics described in Eq. (3). In the aging regime $P_u(t)$ decays towards 0, see Eq. (3) and Fig. 2(b), so that the effective viscosity diverges and the effective elastic modulus decreases towards the value G_0 . For simplicity, in the analytical calculations, we approximate the effective elastic modulus with the value

$G_c \simeq G_0$ to which it converges at long times. This approximation is exact at the lowest order in $P_u(t)$, see Appendix D for details.

III. ACTIVE RHEOLOGY OF AGING CONDENSATES

A. Relaxation function of a Maxwell glass

We now derive and discuss the linear response of a viscoelastic material described by Eqs. (1) and (4) with a constant elastic modulus G_0 . In order to compare our model with rheology experiments, we solve Eq. (4) for the shear stress

$$\sigma(t) = \int_0^t dt' K(t, t') \dot{\epsilon}(t'), \quad (5)$$

where

$$K(t, t') = G_0 e^{-\frac{G_0}{\eta_0} \int_{t'}^t dt'' P_u(t'')} \quad (6)$$

is the relaxation function and $t = 0$ corresponds to the sample preparation time at which $\sigma(0) = 0$.

For $\alpha > 1$, the equilibrium steady state $P_u^{\text{eq}}(t)$ exists and the relaxation function becomes $K(t - t') = G_0 \exp(-P_u^{\text{eq}} G_0 / \eta_0 (t - t'))$. This is the exponential relaxation with the rate $P_u^{\text{eq}} G_0 / \eta_0$, which corresponds to a Maxwell fluid. For $0 < \alpha < 1$, no steady state exists, and the relaxation function exhibits glassy behavior. In the asymptotic regime, $P_u(t)$ follows Eq. (3), from which we obtain

$$K(t, t') \simeq G_0 \exp \left[-\frac{\kappa G_0}{\alpha \Gamma_0 \eta_0} ((\Gamma_0 t)^\alpha - (\Gamma_0 t')^\alpha) \right]. \quad (7)$$

Therefore, in the aging regime, the relaxation function takes the form of a stretched exponential that often appears in the relaxation of glass forming materials [27,28]. Note that the time translational invariance is broken in Eq. (7), a signature of the aging regime. We refer to the relaxation function in Eq. (7) as the relaxation function of an aging Maxwell fluid, i.e., Maxwell glass.

B. Age dependent relaxation time

We consider an experimental protocol where the system is prepared at $t = 0$ and the system is strained starting at the waiting time t_w . The resulting stress is written as

$$\sigma(t) \simeq \int_{t_w}^t dt' K(t, t') \dot{\epsilon}(t'), \quad (8)$$

where $\epsilon(t_w) = 0$. We consider the relaxation function in terms of the observation time $\tau = t - t_w$. In the limit of a short observation time compared to the waiting time $\tau \ll t_w$, the relaxation function $K(t_w + \tau, t_w + \tau')$ can be approximated by a time translation invariant function

$$K_{t_w}(\tau - \tau') \equiv G_0 e^{-\frac{\kappa G_0}{\eta_0} (\Gamma_0 t_w)^{\alpha-1} (\tau - \tau')}. \quad (9)$$

This relaxation function shows that a Maxwell glass behaves as a Maxwell fluid when observed on short times $\tau \ll t_w$, but with age-dependent relaxation time

$$\tau_c(t_w) = \frac{\eta_0}{\kappa G_0} (\Gamma_0 t_w)^{1-\alpha}. \quad (10)$$

The age-dependent Maxwell relaxation time derived here provides a connection between underlying dynamics of the

crosslinker network and Maxwell glass rheology [5]. The aging of the Maxwell relaxation time stems from the stretched exponential relaxation in Eq. (7) that reflects the glassy nature of the material.

C. Instantaneous complex modulus

The relaxation time τ_c in a Maxwell fluid is related to the complex modulus as $G(\omega) = i\omega\tau_c G_0 / (1 + i\omega\tau_c)$ [29]. The complex modulus $G(\omega) = G'(\omega) + iG''(\omega)$, where $G'(\omega)$ and $G''(\omega)$ represent the storage and loss moduli, respectively, characterizes the linear response of a time-translation-invariant material as a function of the angular frequency ω . However, for an aging material, $G(\omega)$ is not a well-defined observable. Nevertheless, a frequency-dependent linear response can still be employed if the observation time window τ is short enough such that the material properties do not undergo significant changes during the observation (Appendix A). To remove the restriction of a short observation time window, which limits the applicability of active rheology for aging material, we now introduce an analytic signal method that allows us to define the instantaneous complex modulus of an aging material $G(\omega, t, t_w)$ at time t and at frequency ω , similar to the time-varying viscoelastic spectrum [21], see Appendix E.

The analytic signal of a function $f(t)$ is defined as $f_a(t) \equiv f(t) + i\mathcal{H}[f(t)](t)$, where \mathcal{H} is the Hilbert transform, see Appendix E. The analytic signal $f_a(t)$ is a complex function and can be written in the polar form, $f_a(t) = |f_a(t)| \exp(i\varphi(t))$, where $|f_a(t)|$ is the instantaneous amplitude, also called envelope, and $\varphi(t) = \arg[f_a(t)]$ is the instantaneous phase of the signal $f(t)$. Using this definition of the analytic signal, we define the instantaneous complex modulus as

$$\begin{aligned} G(\omega, t, t_w) &\equiv \frac{\sigma_a(\omega, t, t_w)}{\epsilon_a(\omega, t)} \\ &= \frac{|\sigma_a(\omega, t, t_w)|}{|\epsilon_a(\omega, t)|} \exp(i\delta\varphi(\omega, t, t_w)), \end{aligned} \quad (11)$$

where $\delta\varphi(\omega, t, t_w)$ is the instantaneous phase difference between shear strain and stress. Here $\sigma_a(\omega, t, t_w)$ is the analytic signal of measured shear stress $\sigma(\omega, t, t_w)$ in response to an imposed sinusoidal shear strain $\bar{\epsilon}(\omega, t, t_w) = \Theta(t - t_w)\epsilon(\omega, t)$ with frequency ω starting at $t = t_w$, where $\epsilon(\omega, t) = \epsilon_0 \cos(\omega t + \varphi_0)$ and Θ is the Heaviside step function. ϵ_0 and φ_0 are the amplitude and initial phase of the shear strain, respectively. The analytical signal of the strain is $\epsilon_a(\omega, t) = \epsilon_0 e^{i(\omega t + \varphi_0)}$. The instantaneous complex modulus $G(\omega, t, t_w)$ is a generalization of the conventional complex modulus $G(\omega)$ to the time dependent signals and they become equal for a time translation invariant system, see Appendix E. It reduces to the time-varying viscoelastic spectrum defined in Ref. [21] for slow aging limit as discussed in Appendix E.

We use the instantaneous complex modulus to analyze the rheology of our model. For simplicity we choose a waiting time $t_w = 0$, which does not affect the aging process in our model. We, therefore, omit the t_w dependence in the following. We solve Eq. (4) with Eq. (1) numerically for the sinusoidal shear strain as input $\bar{\epsilon}(\omega, t)$ and obtain the shear stress $\sigma(\omega, t)$ as output. Figure 3(a) shows the shear strain and stress for $\omega = \pi/10$ and $\omega = \pi/100$ for $\alpha = 10$ and

$\alpha = 0.5$, respectively. For $\alpha = 10$, the strain is stationary, reflecting the equilibrium viscosity in Eq. (4). In contrast, for $\alpha = 0.5$ the amplitude of shear stress increases in time due to aging, reflected in changing viscosity $\eta_0/P_u(t)$. In Fig. 3(b), we calculate the real and imaginary part of the instantaneous complex modulus, $G'(\omega, t)$ and $G''(\omega, t)$, respectively, for a range of input frequencies. For $\alpha = 10$, $G(\omega, t)$ does not depend on the time. On the contrary, we observe a striking difference for $\alpha = 0.5$: the instantaneous complex modulus shifts to lower frequencies over time, showing that the characteristic relaxation time of the material increases, as shown in Fig. 3(b), right panel. Such aging behavior was observed experimentally in the protein condensates [5]. Moreover, Jawerth *et al.* [5] demonstrated that experimentally measured complex moduli in the Maxwell glass collapse when rescaled by G_c and frequencies by ω_c , where G_c and ω_c are defined by $G'(\omega_c, t) = G''(\omega_c, t) = G_c$. We show in Fig. 3(c) that our numerically evaluated complex moduli indeed collapse on a single master curve of the Maxwell fluid when rescaled moduli and frequency by G_c and ω_c , respectively.

IV. FLUCTUATION-RESPONSE RELATIONS IN AGING CONDENSATES

In an equilibrium system, the relaxation of spontaneous fluctuations and the linear response to an external perturbation are closely related by the fluctuation-dissipation theorem [30]. Using the generalized Stokes-Einstein relation derived from the fluctuation-dissipation theorem, rheological properties of the material can be determined from equilibrium fluctuations [5,31]. Although the equilibrium fluctuation-response relations do not apply in the aging materials, we derive specific fluctuation-response relations that characterize the aging Maxwell fluid.

To this end, we consider a spatially resolved version of Eq. (1) that takes into account diffusion of unbound elements

$$\frac{1}{\Gamma_0} \frac{\partial p_b(x, E, t)}{\partial t} = -p_b(x, E, t)e^{-\beta E} + p_u(x, t)\rho(E), \quad (12a)$$

$$\begin{aligned} \frac{1}{\Gamma_0} \frac{\partial p_u(x, t)}{\partial t} &= \frac{D_0}{\Gamma_0} \frac{\partial^2 p_u(x, t)}{\partial x^2} - p_u(x, t) \\ &+ \int_0^\infty dE p_b(x, E, t)e^{-\beta E}, \end{aligned} \quad (12b)$$

with the initial condition $p_b(x, E, 0) = 0$ and $p_u(x, 0) = \delta(x)$. In Eq. (12), $p_b(x, E, t)$ is the probability density of elements bound at position x with energy E at time t and $p_u(x, t)$ is the density of diffusing elements at position x at time t .

The mean-square displacement of fluctuating elements is

$$\langle \Delta x^2 \rangle(t) = \Delta_u(t) + \int_0^\infty dE \Delta_b(E, t), \quad (13)$$

where we have defined the positional variance of diffusing and bound states, respectively, as

$$\begin{aligned} \Delta_u(t) &\equiv \int_{-\infty}^\infty dx x^2 p_u(x, t); \\ \Delta_b(E, t) &\equiv \int_{-\infty}^\infty dx x^2 p_b(x, E, t). \end{aligned} \quad (14)$$

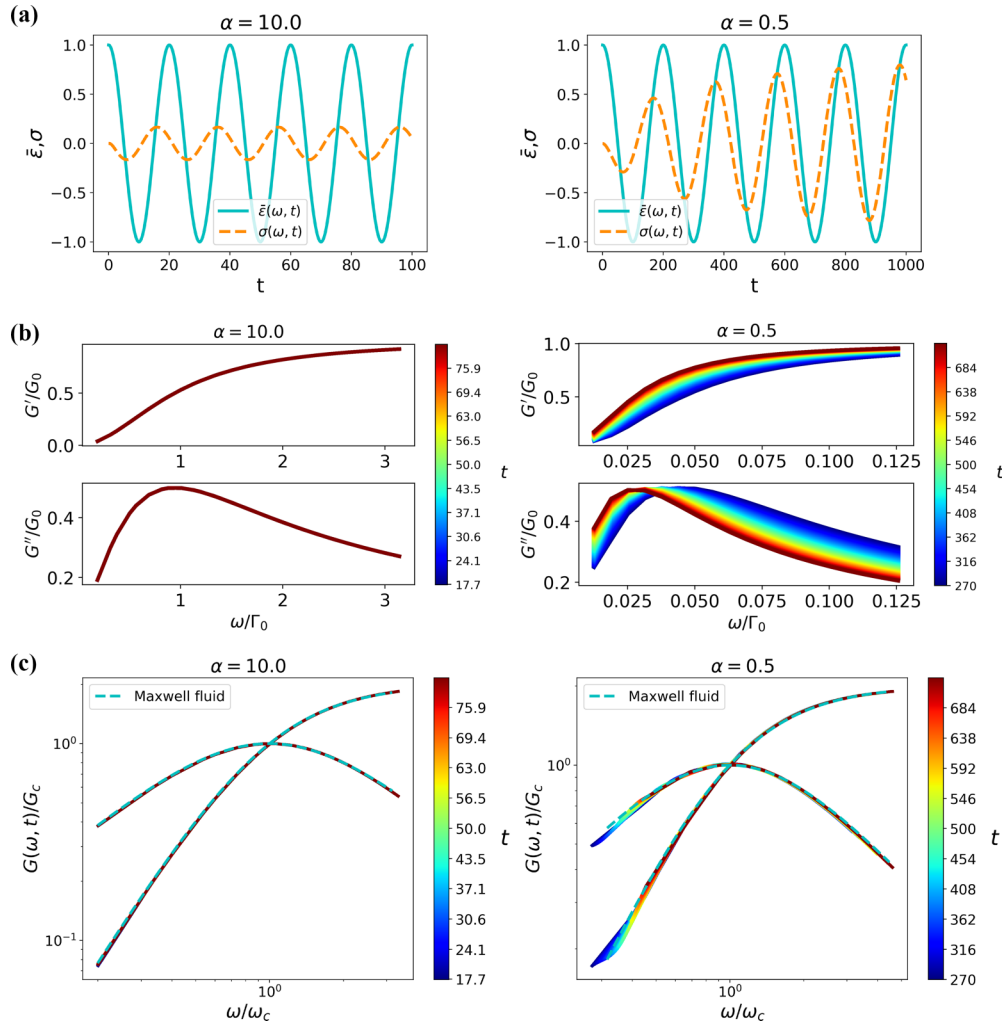


FIG. 3. Active rheology for the Maxwell fluid and glass. In the case of $\alpha = 10.0$ the system has a stationary equilibrium state and thus behave as conventional Maxwell fluid. For $\alpha = 0.5$, the system shows aging, thus behaving as the Maxwell glass. The unit time is $1/\Gamma_0$ in Eq. (1). (a) The input shear strain $\bar{\epsilon}(\omega, t)$ (cyan solid line) and the output shear stress $\sigma(\omega, t)$ (orange dashed lines). $\omega = \pi/10$ for $\alpha = 10.0$ and $\omega = \pi/100$ for $\alpha = 0.5$. (b) The instantaneous complex modulus $G(\omega, t)$ in equilibrium and aging regime. The real and imaginary part of $G(\omega, t)$ is $G'(\omega, t)$ and $G''(\omega, t)$, respectively. (c) The collapse of the $G(\omega, t)$ for different instances onto the single master curve of the Maxwell fluid (dashed line in cyan). The bare viscosity is set to $\eta_0 = 0.5$. We fix β_0 to 1 and vary β . Detailed numerical procedures are in Appendix H.

Using Eqs. (12) and (14), we obtain the time evolution of the mean-squared displacement,

$$\frac{1}{\Gamma_0} \frac{\partial \Delta_b(E, t)}{\partial t} = -\Delta_b(E, t)e^{-\beta E} + \Delta_u(t)\rho(E), \quad (15a)$$

$$\begin{aligned} \frac{1}{\Gamma_0} \frac{\partial \Delta_u(t)}{\partial t} &= 2\frac{D_0}{\Gamma_0} P_u(t) - \Delta_u(t) \\ &+ \int_0^\infty dE \Delta_b(E, t)e^{-\beta E}, \end{aligned} \quad (15b)$$

with the definition,

$$P_u(t) \equiv \int_{-\infty}^\infty dx p_u(x, t). \quad (16)$$

The expression for the effective diffusion coefficient, $D(t)$, can be obtained by taking the time derivative of Eq. (13) and

using Eq. (15),

$$\frac{d}{dt} \langle \Delta x^2 \rangle(t) = 2D_0 P_u(t), \quad (17)$$

leading to

$$D(t) \equiv D_0 P_u(t). \quad (18)$$

Equation (17) states that the effective diffusion coefficient is proportional to the probability that the element being in the diffusive state.

We now obtain a relation between the aging relaxation function and the mean-squared displacement at different times using Eqs. (6) and (17)

$$K(t, t') = G_0 \exp\left(-\frac{G_0}{2D_0\eta_0} (\langle \Delta x^2 \rangle(t) - \langle \Delta x^2 \rangle(t'))\right). \quad (19)$$

This exact relation connects the time dependent rheology $K(t, t')$ of the Maxwell glass to the passive rheology

characterised by the mean-squared displacement $\langle \Delta x^2 \rangle(t)$. Alternatively, we can write the second relation between mean-squared displacement and linear response function. Using the strain-stress response function $\chi(t, t')$ defined as

$$\epsilon(t) = \int_0^t \chi(t, t') \sigma(t'), \quad (20)$$

we obtain (see Appendix F)

$$\Theta(t - t') \frac{d}{dt'} \langle \Delta x^2(t') \rangle = 2k_B T \chi(t, t'). \quad (21)$$

Equation (21) stems from the fact that both the time dependence of the diffusion coefficient $D(t)$ and of the active response given in Eq. (4) are governed by $P_u(t)$. We have used $D_0 = k_B T / \eta_0$ implying that diffusion coefficient of the unbound elements satisfies the Einstein relation. Note that Eq. (21) is similar to but different from the time translation invariant fluctuation dissipation theorem in equilibrium. It applies to the aging Maxwell model and has both t and t' dependence signifying the glassy behavior.

V. DISCUSSION

We have presented a mean-field model of aging biological condensates, based on a minimal trap model that exhibits glassy behavior [24]. Our model recapitulates aging rheology recently observed in biological condensates termed Maxwell glass. A Maxwell glass exhibits at all times Maxwell fluid behavior with an age-dependent relaxation time, correspondingly the viscosity is age dependent and diverges for long times, even though the system remains fluid. In addition, it was observed that the elastic modulus decreased slightly but remained roughly constant [5]. Interestingly the complex modulus measured at different ages collapses on master curves describing a Maxwell fluid. In the aging regime of our model the fraction of unbound elements decays with time as a power law $P_u(t) \sim t^{\alpha-1}$ ($\alpha < 1$). This leads to a diverging effective viscosity $\eta_0/P_u(t)$ and a weakly decreasing effective modulus $G_0/(1 - P_u(t))$ that approaches a finite value. The relaxation function $K(t, t')$ in our model exhibits a stretched exponential that decays at low temperatures, a characteristic for glassy systems. The resulting Maxwell relaxation time is age dependent and increases with waiting time t_w as a power law $\tau_c \sim t_w^{1-\alpha}$. The complex modulus determined in our model collapses on curves describing a Maxwell model, consistent with experiment.

For such an aging material for which time translation invariance is not obeyed, defining the frequency dependent complex modulus poses a challenge. To overcome this challenge, we introduce the time-dependent instantaneous complex modulus as a generalization of the conventional complex modulus at steady state. The instantaneous complex modulus is based on analytic signal construction and remains well-defined even in nonstationary systems where approximative measures of the conventional complex modulus would fail.

Our theory is a phenomenological mean-field model that captures key characteristic rheological properties of protein condensates [5]. Different future extensions of our study will be of interest. These include a microscopic model of the protein condensate network, for example by building on models

for dynamic crosslinked networks such as Flory's addition-subtraction network theory [32,33] and transient network theory [34,35]. Moreover, another interesting extension would be to consider the coupling between externally applied shear stress and the unbinding rate of crosslinked proteins. This could potentially provide insight into plastic events, a phenomenon that has been investigated within the context of amorphous materials [36,37] and particularly in connection to aging [38].

A power-law dependence of the relaxation time on the waiting time has been observed in a different system. The aging exponent μ , which describes the growth of relaxation time with waiting time as $\tau_c \sim t_w^\mu$ has been introduced in the seminal work [19]. In many polymeric materials, the relaxation time grows sublinearly, $\mu \simeq 0.5-1$ [10]. In our model $\mu = 1 - \alpha$ [see Eq. (10)] and in the aging regime with $0 < \alpha < 1$, we find a sublinear dependence of τ_c on t_w for a Maxwell glass, consistent with the sublinear behavior seen in many experiments on nonbiological materials.

Interestingly, recent experiments suggest that μ could be larger than 1 in protein condensates. For example, for the PGL-3 protein, $\mu \simeq 6.4$ and $\mu \simeq 2.1$ were estimated for different salt conditions (150 mM KCl and 100 mM KCl, respectively) [5]. Our current model does not account for such high values of μ , as they would require negative values of α and we currently do not have an explanation of this discrepancy. There are only very few other systems where $\mu > 1$ was measured. An example is polycarbonate (see for instance Fig. 15 in [19]). Further research will be required to find out whether $\mu > 1$ is a robust feature of biological protein condensates, and if so, what is the origin of such a different behavior in comparison to aging of non-biological polymers. One possible explanation of the rapid aging observed in protein condensates, is that the system may not yet be exploring the tail of the distribution $\rho(E)$ for large E within the experimental time scales. Instead, the system may be exploring smaller E , where the distribution $\rho(E)$ might not be a decreasing function of E . This could lead transiently to a relaxation time that grows exponentially with age. The functional form of the distribution $\rho(E)$ could be probed experimentally, for example, through a measurement of the distribution of protein trapping times.

Finally, we have obtained an exact relation between the relaxation function and the mean-squared displacement of particles in the aging regime [Eq. (19)]. This relation is similar to the fluctuation-dissipation theorem that holds for equilibrium systems but it applies to the out-of-equilibrium Maxwell glass. In out-of-equilibrium aging systems, the generalized fluctuation-dissipation theorem has been hypothesized and verified for various models, resulting in the definition of an effective temperature [39-41]. The fluctuation-response relation, given by Eq. (21), does not require an effective temperature. Instead, it directly connects the response function to the fluctuations observed in Maxwell glass.

ACKNOWLEDGMENTS

R.T. thanks to the overseas research fellowship No. 202260312 from the Japan Society for the Promotion of Science. The authors thank Lars Hubatsch for the valuable comments.

APPENDIX A: RHEOLOGY OF GLASSY MATERIALS

Soft materials, including protein condensates, behave as viscoelastic fluids. We consider a material that was prepared at $t = 0$ and start measuring the material properties after a waiting time, $t = t_w$. Linear viscoelasticity is characterized by the linear constitutive relation between stress (σ) and strain (ϵ). We consider the stress and strain relative to $t = 0$, which subsume the effect of stress and strain at $t = 0$ into $\sigma(t)$ and $\epsilon(t)$, respectively. The linear constitutive relation reads

$$\sigma(t) = \int_0^t G(t, t') \epsilon(t') dt', \quad (\text{A1})$$

where we consider a general case without time translation symmetry [21]. Here, $G(t, t')$ is dynamic modulus determining the linear relation between the shear strain and stress. We can alternatively write the relation between stress and strain rate,

$$\sigma(t) = \int_0^t K(t, t') \dot{\epsilon}(t') dt', \quad (\text{A2})$$

where $\dot{\epsilon}$ is the rate of deformation. $K(t, t')$ is called relaxation function. We obtain the relation between $G(t, t')$ and $K(t, t')$ by applying partial integration to Eq. (A2),

$$G(t, t') = -\frac{dK(t, t')}{dt'} + 2\delta(t - t')K(t, t'). \quad (\text{A3})$$

The factor 2 in the above relation is to account for the delta function integrated at the boundary. We used the fact that $\epsilon(0) = 0$. We can also write the linear relationship between stress and strain using the response function, $\chi(t, t')$,

$$\epsilon(t) = \int_0^t \chi(t, t') \sigma(t') dt'. \quad (\text{A4})$$

When the probing material is in thermodynamic equilibrium and independent on initial conditions, the above response functions depend only on the time interval $t - t'$: $G(t - t')$, $K(t - t')$, and $\chi(t - t')$, corresponding to the time translational invariance. Time translational invariance allows us to apply the convolution theorem for the Laplace transform to Eq. (A1)–(A4), leading to the simple expressions:

$$\sigma(s) = G(s)\epsilon(s); \quad (\text{A5})$$

$$\sigma(s) = sK(s)\epsilon(s); \quad (\text{A6})$$

and

$$\epsilon(s) = \chi(s)\sigma(s). \quad (\text{A7})$$

We specified the quantities in the Laplace space by the argument s . We use same convention to denote the quantities in Laplace space (s) and in Fourier space (ω). Therefore the response functions have relation $G(s) = sK(s) = 1/\chi(s)$ when time translational invariance is satisfied. For causal functions, such as $G(t, t')$, $K(t, t')$, and $\chi(t, t')$, the Fourier transform is readily obtained from the Laplace transform, by analytic continuation: $s \rightarrow i\omega$. Thus, the analytic continuation may give the equivalent relation in the Fourier space, $G(\omega) = i\omega K(\omega) = 1/\chi(\omega)$.

The dynamic modulus in Fourier space $G(\omega)$, is often referred to as complex modulus [17]:

$$G(\omega) = G'(\omega) + iG''(\omega), \quad (\text{A8})$$

where the real part $G'(\omega)$ is the storage modulus, and the imaginary part $G''(\omega)$ is the loss modulus. The storage modulus and the loss modulus reflect the elastic and viscous component of the material response, respectively. The moduli $G'(\omega)$ and $G''(\omega)$ may be obtained using active rheology. Depending on the experimental setup, we can choose either strain or stress as input and output signal. Here, we choose, strain as the input and stress as the output. Using a sinusoidal input strain with frequency ω , and amplitude $\epsilon(\omega)$, one can determine the moduli by measuring the steady-state output stress, $\sigma(\omega)$, from the amplitude change and the phase shift:

$$G'(\omega) = \frac{\sigma(\omega)}{\epsilon(\omega)} \cos(\delta\varphi(\omega)); \quad (\text{A9a})$$

$$G''(\omega) = \frac{\sigma(\omega)}{\epsilon(\omega)} \sin(\delta\varphi(\omega)), \quad (\text{A9b})$$

where $\delta\varphi$ is the phase difference between input and output sinusoidal signals.

In contrast to a material at thermodynamic equilibrium, glassy material, on the other hand, violates time translational invariance due to the slow relaxation which implies that memory about the initial state is not lost. The consequence is the explicit dependence on the two time scales in the complex modulus and the relaxation function, $G(t, t')$ and $K(t, t')$. We introduce the waiting time (t_w), the time between the preparation of the material ($t = 0$) and the start of the measurement, and the observation time τ during measurement, such that the time is $t = t_w + \tau$. With the strain imposed starting at $t = t_w$, Eq. (A1) becomes

$$\sigma(t) = \int_{t_w}^t G(t, t') \epsilon(t') dt'. \quad (\text{A10})$$

Using the change of variables, $\tau = t - t_w$ and $\tau' = t' - t_w$,

$$\sigma(t_w + \tau) = \int_0^\tau G(t_w + \tau, t_w + \tau') \epsilon(t_w + \tau') d\tau'. \quad (\text{A11})$$

One approach to circumvent the complexity of the two time scales is to use observation times τ much smaller than time scale associated with the change in rheological properties. For such a measurement time, $G(t_w + \tau, t_w + \tau') \simeq G(t_w, t_w + \tau' - \tau)$ obeys time translational invariance for τ . We denote the resulting dynamic modulus as $G_{t_w}(\tau - \tau') \equiv G(t_w, t_w + \tau' - \tau)$. Then Eq. (A11) is approximated as

$$\sigma_{t_w}(\tau) \simeq \int_0^\tau G_{t_w}(\tau - \tau') \epsilon_{t_w}(\tau') d\tau', \quad (\text{A12})$$

where $\sigma_{t_w}(\tau) \equiv \sigma(t_w + \tau)$ and $\epsilon_{t_w}(\tau) \equiv \epsilon(t_w + \tau)$. Once we approximate the modulus to have time translational invariance for τ , one can obtain the storage and loss modulus for waiting time $t = t_w$ using the same procedure as for the equilibrium case. Repeating this procedure for different t_w , we obtain the t_w -dependent material properties. We remark that the assumption that the observation time τ is appreciably smaller than the dynamics of the glassy material is not *a priori* justified and must be checked posteriorly.

An alternative way to obtain the time-dependent material properties during aging, which does not require repeated analysis for different waiting times t_w , is to generalize the complex modulus $G(\omega)$ to time-dependent spectra [21] (Appendix E).

The viscoelastic spectra explicitly represent the time-varying material properties, but their computation from experiments is not straightforward. We introduce, in Sec. III C, the instantaneous complex modulus to characterize the rheology of aging materials. We show in Appendix E that the instantaneous complex modulus and the viscoelastic spectra are closely related. The instantaneous complex modulus does not require the assumption for the observation time scale and thus captures the full spectrum of the aging material.

APPENDIX B: DECOMPOSITION IN DYNAMIC MODES

We study the relaxation dynamics of Eq. (1) to the asymptotic solutions for equilibrium and aging regime by defining eigenmodes and eigenvalues. First, we make the transformation $q_b(E, t) = p_b(E, t)e^{-\beta E/2}/\sqrt{\rho(E)}$, to transform the operator Hermitian, and rewrite Eq. (1) as

$$\frac{1}{\Gamma_0} \frac{\partial q_b(E, t)}{\partial t} = -q_b(E, t)e^{-\beta E} + P_u(t)\sqrt{\rho(E)}e^{-\beta E/2}, \quad (\text{B1a})$$

$$\frac{1}{\Gamma_0} \frac{\partial P_u(t)}{\partial t} = -P_u(t) + \int_0^\infty dE q_b(E, t)\sqrt{\rho(E)}e^{-\beta E/2}. \quad (\text{B1b})$$

We introduce eigenfunctions $q_\lambda^b(E)$ and P_λ^u of the linear operator defined in Eq. (B1). These eigenfunctions obey

$$-\frac{1}{\Gamma_0} \lambda q_\lambda^b(E) = -q_\lambda^b(E)e^{-\beta E} + \sqrt{\rho(E)}e^{-\beta E/2} P_\lambda^u, \quad (\text{B2a})$$

$$-\frac{1}{\Gamma_0} \lambda P_\lambda^u = -P_\lambda^u + \int_0^\infty dE \sqrt{\rho(E)} q_\lambda^b(E) e^{-\beta E/2}, \quad (\text{B2b})$$

where λ denotes the corresponding eigenvalue.

We can eliminate q_λ^b from Eq. (B2) which leads to the condition

$$\left(1 - \frac{1}{1 - \lambda/\Gamma_0} \int_0^\infty dE \frac{\rho(E)e^{-\beta E}}{e^{-\beta E} - \lambda/\Gamma_0}\right) P_\lambda^u = 0. \quad (\text{B3})$$

In order to find the eigenfunctions, we distinguish two cases.

Case (I): $P_\lambda^u = 0$. In this case Eq. (B2) reduces to

$$-\frac{1}{\Gamma_0} \lambda q_\lambda^b(E) = -q_\lambda^b(E)e^{-\beta E}, \quad (\text{B4a})$$

$$0 = \int_0^\infty dE \sqrt{\rho(E)} q_\lambda^b(E) e^{-\beta E/2}. \quad (\text{B4b})$$

This can be solved by the ansatz, $q_\lambda^b(E) = a\delta(E - E_\lambda) + \delta'(E - E_\lambda)$, where a is a constant. From Eq. (B4b) we obtain

$$a = \frac{\beta - \beta_0}{2}, \quad (\text{B5})$$

leading to

$$q_\lambda^b(E) = \frac{\beta - \beta_0}{2} \delta(E - E_\lambda) + \delta'(E - E_\lambda), \quad (\text{B6})$$

with the eigenvalues, $\lambda = \Gamma_0 e^{-\beta E}$.

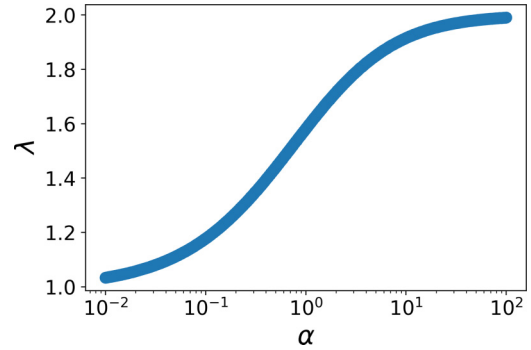


FIG. 4. Eigenvalue λ as a function of α obtained by numerically solving Eq. (B8). Γ_0 is set to unity. λ determines the relaxation rate to the asymptotic solutions in equilibrium and aging regime (see Fig. 2).

Case (II): $P_\lambda^u \neq 0$ and $\int_0^\infty dE \frac{\rho(E)e^{-\beta E}}{e^{-\beta E} - \lambda/\Gamma_0} = 1 - \lambda/\Gamma_0$. Using the variable transform $x = e^{-\beta E}$, we find

$$\begin{aligned} & \int_0^\infty dE \frac{\rho(E)e^{-\beta E}}{e^{-\beta E} - \lambda/\Gamma_0} \\ &= \frac{\beta_0}{\beta} \int_0^1 dx \frac{x^{\frac{\beta_0}{\beta}}}{x - \lambda/\Gamma_0} \\ &= -\frac{\beta_0}{\beta} \frac{\Gamma_0}{(1 + \beta_0/\beta)\lambda^2} {}_2F_1\left(1, \frac{\beta_0}{\beta} + 1, \frac{\beta_0}{\beta} + 2, \frac{\Gamma_0}{\lambda}\right), \end{aligned} \quad (\text{B7})$$

where ${}_2F_1$ is the Hypergeometric function [42]. Therefore the corresponding eigenvalue obeys the equation:

$$\frac{\alpha}{1 + \alpha^2} {}_2F_1\left(1, \alpha + 1, \alpha + 2, \frac{\Gamma_0}{\lambda}\right) = \frac{\lambda}{\Gamma_0} \left(\frac{\lambda}{\Gamma_0} - 1\right), \quad (\text{B8})$$

where $\alpha = \beta_0/\beta$. Because $P_\lambda^u = 0$ for case (I), the relaxation dynamics of $P_u(t)$ is fully determined by the eigenvalue satisfying Eq. (B8), which depends on α . Figure 4 shows the eigenvalue λ as a function of α .

APPENDIX C: SOLUTIONS OF DYNAMIC EQUATIONS USING LAPLACE TRANSFORMS

In this Appendix, we solve Eq. (1) using the Laplace transform and obtain asymptotic solutions for long time. Because of the conservation of probabilities, $P_u(t) + \int_0^\infty dE' p_b(E', t) = 1$, Eq. (1) can be written in one equation,

$$\begin{aligned} & \frac{1}{\Gamma_0} \frac{d}{dt} p_b(E, t) = -e^{-\beta E} p_b(E, t) \\ & - \rho(E) \int_0^\infty p_b(E', t) dE' + \rho(E). \end{aligned} \quad (\text{C1})$$

We take the Laplace transform of Eq. (C1) with respect to t and solve for $p_b(E, s)$,

$$\begin{aligned} p_b(E, s) &= -\frac{\rho(E)C(s)}{s/\Gamma_0 + e^{-\beta E}} + \frac{p_b(E, 0)/\Gamma_0}{s/\Gamma_0 + e^{-\beta E}} \\ &+ \frac{\rho(E)}{(s/\Gamma_0 + e^{-\beta E})s}, \end{aligned} \quad (\text{C2})$$

where

$$C(s) = \frac{\int_0^\infty dE' \frac{p_b(E', 0)/\Gamma_0 +}{s/\Gamma_0 + e^{-\beta E'}} + \int_0^\infty dE' \frac{\rho(E')}{(s/\Gamma_0 + e^{-\beta E'})s}}{1 + \int_0^\infty dE' \frac{\rho(E')}{s/\Gamma_0 + e^{-\beta E'}}}. \quad (\text{C3})$$

Equations (C2) and (C3) with $P_u(s) = 1/s - \int_0^\infty dE p_b(E, s)$ give the complete solution of Eq. (1) in Laplace space.

We first derive the expression of $P_u(s)$ for $s \rightarrow 0$. Integrating Eq. (C2) for E to obtain

$$P_b(s) = -C(s)Q_\rho(s) + Q_0(s) + \frac{1}{s}Q_\rho(s), \quad (\text{C4})$$

where

$$Q_\rho(s) \equiv \int_0^\infty dE \frac{\rho(E)}{s/\Gamma_0 + e^{-\beta E}}; \quad (\text{C5})$$

$$Q_0(s) \equiv \int_0^\infty dE \frac{p_b(E, 0)/\Gamma_0}{s/\Gamma_0 + e^{-\beta E}}; \quad (\text{C6})$$

and

$$C(s) = \frac{Q_\rho(s)}{s(1 + Q_\rho(s))} + \frac{Q_0(s)}{1 + Q_\rho(s)}. \quad (\text{C7})$$

$P_b(s)$ simplifies to

$$P_b(s) = \frac{Q_\rho(s)}{s(1 + Q_\rho(s))} + \frac{Q_0(s)}{1 + Q_\rho(s)}, \quad (\text{C8})$$

and

$$\begin{aligned} P_u(s) &= \frac{1}{s} - P_b(s) \\ &= \frac{1}{s} \frac{1}{1 + Q_\rho(s)} - \frac{Q_0(s)}{1 + Q_\rho(s)}. \end{aligned} \quad (\text{C9})$$

The term containing $Q_0(s)$ in the second line of Eq. (C9) is the contribution from the initial distribution giving subordinate contribution for long time. Here it is set to 0 because $p_b(E, 0) = 0$, leading to

$$P_u(s) = \frac{1}{s} \frac{1}{1 + Q_\rho(s)}. \quad (\text{C10})$$

One can explicitly evaluate $Q_\rho(s)$ for $s \rightarrow 0$ as follows for equilibrium case (I) and aging case (II).

Equilibrium case (I). For the equilibrium case one can expand $Q_\rho(s)$ as follows for $s \rightarrow 0$,

$$\begin{aligned} Q_\rho(s) &= \int_0^\infty dE \frac{\beta_0 e^{-\beta_0 E}}{s/\Gamma_0 + e^{-\beta E}} \\ &\simeq \frac{\beta_0}{\beta_0 - \beta} - \frac{s}{\Gamma_0} \frac{\beta_0}{\beta_0 - 2\beta} + O(s^2). \end{aligned} \quad (\text{C11})$$

We substitute the first term of the expansion into Eq. (C10) to obtain

$$P_u(s) \simeq \frac{\beta_0/\beta - 1}{s(2\beta_0/\beta - 1)}. \quad (\text{C12})$$

Inverting to the real space, we have

$$P_u^{eq} = \frac{\alpha - 1}{2\alpha - 1}, \quad (\text{C13})$$

where $\alpha = \beta_0/\beta > 1$.

Aging case (II). For the aging case, we first make variable transforms to extract the power law form of s :

$$\begin{aligned} Q_\rho(s) &= \int_0^\infty dE \frac{\beta_0 e^{-\beta_0 E}}{s/\Gamma_0 + e^{-\beta E}} \\ &= \frac{\beta_0}{\beta} \int_0^1 dx \frac{x^{\frac{\beta_0}{\beta} - 1}}{s/\Gamma_0 + x} \\ &= \frac{\beta_0}{\beta} \left(\frac{s}{\Gamma_0} \right)^{\frac{\beta_0}{\beta} - 1} \int_0^{\Gamma_0/s} dy \frac{y^{\frac{\beta_0}{\beta} - 1}}{1 + y}. \end{aligned} \quad (\text{C14})$$

In the second line, we used the change of variables $x = e^{-\beta E}$ and the third line, $y = x\Gamma_0/s$. In the limit of $s \rightarrow 0$, we can extend the upper bound of the integral in the third line to ∞ :

$$\int_0^\infty dy \frac{y^{\frac{\beta_0}{\beta} - 1}}{1 + y} = \pi \csc \left(\frac{\beta_0}{\beta} \pi \right). \quad (\text{C15})$$

Thus, in the limit of $s \rightarrow 0$,

$$Q_\rho(s) \simeq \frac{\beta_0}{\beta} \left(\frac{s}{\Gamma_0} \right)^{\frac{\beta_0}{\beta} - 1} \pi \csc \left(\frac{\beta_0}{\beta} \pi \right). \quad (\text{C16})$$

Noting that $\beta_0/\beta - 1 < 0$ in the aging regime, $1 + Q_\rho(s) \simeq Q_\rho(s)$ for $s \rightarrow 0$. From Eq. (C10),

$$P_u(s) \simeq \frac{1}{sQ_\rho(s)} = \frac{\beta\Gamma_0 \sin \left(\frac{\beta_0}{\beta} \pi \right)}{\beta_0(s/\Gamma_0)^{\frac{\beta_0}{\beta}} \pi}. \quad (\text{C17})$$

By taking the inverse Laplace transform we obtain the result for long time

$$P_u(t) = \frac{\sin(\alpha\pi)}{\alpha\pi\Gamma[\alpha]} (\Gamma_0 t)^{\alpha-1}, \quad (\text{C18})$$

where $\alpha = \beta_0/\beta < 1$.

One can find complete solutions for special cases, infinite temperature ($\beta = 0$) and zero temperature ($\beta = \infty$). For the infinite temperature case, solving Eqs. (C2) and (C3) and taking the inverse Laplace transform, we obtain,

$$\begin{aligned} P_b(t) &= \frac{1}{2}(1 + e^{-2\Gamma_0 t}(-1 + 2P_b(0))), \\ P_u(t) &= \frac{1}{2}(1 - e^{-2\Gamma_0 t}(-1 + 2P_b(0))). \end{aligned} \quad (\text{C19})$$

For the zero temperature case, solving Eqs. (C2) and (C3) and taking inverse Laplace transform, we obtain,

$$\begin{aligned} P_b(t) &= 1 - P_u(0)e^{-\Gamma_0 t}, \\ P_u(t) &= P_u(0)e^{-\Gamma_0 t}. \end{aligned} \quad (\text{C20})$$

This suggests that the dynamics is completely frozen for zero temperature.

APPENDIX D: CHANGE OF ELASTICITY IN AGING REGIME

In the aging regime the fraction of the bound crosslinker ($1 - P_u(t)$) quickly converges towards 1. This can be substantiated by the numerical values of $P_u(t)$ presented in Fig. 2(b), which are several orders of magnitude smaller than 1. In the equilibrium regime, the $P_u(t)$ value is constant, and so any change to G_0 would also be constant. As such, the effect of ($1 - P_u(t)$) on the modulus G_0 does not alter the overall

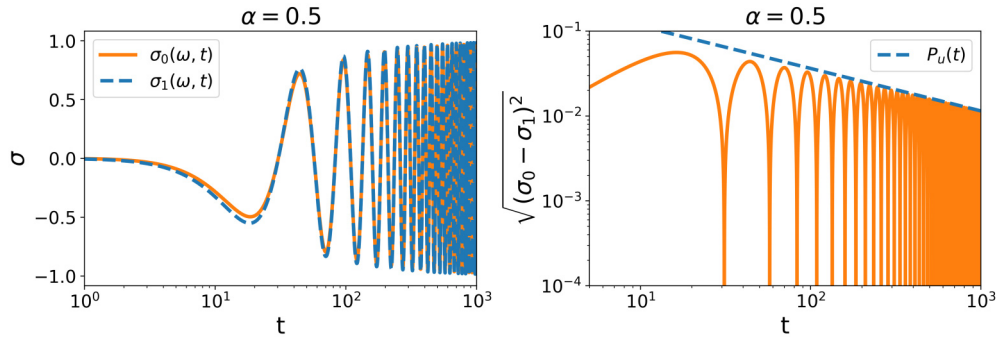


FIG. 5. Left: Comparison of the resulting stresses σ_1 and σ_0 obtained from the model with effective elastic modulus $G_c = G_0/(1 - P_u(t))$ (blue dashed line) and $G_c = G_0$ (orange solid line), respectively. The value of frequency $\omega = \pi/5$ used in this example is the highest frequency presented in Fig. 3, for which the difference between σ_1 and σ_0 is most pronounced. Right: The square root of difference between σ_1 and σ_0 . The dashed line is $P_u(t)$ determining the decay of the difference.

behavior of the system. We numerically test the effect of the correction term $P_u(t)$ by imposing a periodic shear strain in the model with $G_c = G_0/(1 - P_u(t))$ and $G_c = G_0$, and calculating the resulting stresses, see Fig. 5. We find that the magnitude of difference between the two stresses is bounded by $P_u(t) \rightarrow 0$.

APPENDIX E: HILBERT TRANSFORM, ANALYTIC SIGNAL, AND RHEOLOGY

We refer to Refs. [43,44] for the theory and various applications with a comprehensive table of Hilbert transform. We discuss here the basic definition of Hilbert transform and analytic signal, and the connection to rheology. The Hilbert transform of a function, $f(t)$, is defined as

$$\mathcal{H}[f](t) = \frac{1}{\pi} p.v. \int_{-\infty}^{\infty} \frac{f(t')}{t - t'} dt', \quad (\text{E1})$$

where *p.v.* denotes Cauchy principle value. Fourier transform (\mathcal{F}) of Hilbert transformed signal is the ± 90 degrees phase shift, depending on the sign of the frequency ω , of the original signal, namely,

$$\mathcal{F}[\mathcal{H}[f]](\omega) = -i \text{sgn}(\omega) \mathcal{F}[f](\omega), \quad (\text{E2})$$

where *sgn* is signum function. Using the Hilbert transform, analytic representation of $f(t)$ is

$$f_a(t) = f(t) + i\mathcal{H}[f](t). \quad (\text{E3})$$

In the context of the active rheology of aging material, the following theorem is useful.

Bedrosian's theorem [45]: Suppose a low-pass signal, $l(t)$, and high-pass signal, $h(t)$, have Fourier transforms $L(\omega)$ and $H(\omega)$, respectively, where $L(\omega) = 0$ for $|\omega| > \omega_0$ and $H(\omega) = 0$ for $|\omega| < \omega_0$. Then,

$$\mathcal{H}[l(t)h(t)] = l(t)\mathcal{H}[h(t)]. \quad (\text{E4})$$

Namely, the product of a low-pass and a high-pass signal with nonoverlapping spectra is obtained by the product of the low-pass signal and the Hilbert transform of the high-pass signal. In the context of rheology, Bedrosian's theorem requires the

spectra of the aging to have a maximum spectrum smaller than the frequency of input sinusoidal shear strain.

Time-varying viscoelastic spectrum. We illustrate the connection of the analytic signal to the time-dependent rheology of aging materials. Let us consider the relation between the stress and strain rate of a material with a relaxation function $K(t, t')$:

$$\sigma(t) = \int_0^t K(t, t') \dot{\epsilon}(t') dt'. \quad (\text{E5})$$

We apply the sinusoidal strain having frequency ω starting at $t = t_w$: $\bar{\epsilon}(\omega, t, t_w) = \Theta(t - t_w)\epsilon(t)$ where $\epsilon(t) = \Re[\epsilon_0 e^{i(\omega t + \varphi_0)}]$ and $\Theta(t)$ is Heaviside step function. Substituting $\epsilon(\omega, t, t_w)$ to Eq. (E5) leads to

$$\sigma(\omega, t, t_w) = \Re[\epsilon_0 e^{i(\varphi_0 + \omega t)} G^*(\omega, t, t_w)], \quad (\text{E6})$$

where

$$G^*(\omega, t, t_w) \equiv i\omega \int_{t_w}^t e^{-i\omega(t-t')} K(t, t') dt' + e^{-i\omega(t-t_w)} K(t, t_w). \quad (\text{E7})$$

$G^*(\omega, t, t_w)$ is the time-varying viscoelastic spectrum [21].

We show that the time-varying viscoelastic spectrum may be obtained from the method of analytic signal. The analytic signal of the input strain, $\Re[\epsilon_0 e^{i(\omega t + \varphi_0)}]$, is $\epsilon_a(t) = \epsilon_0 e^{i(\omega t + \varphi_0)}$. Taking the Hilbert transform of Eq. (E6),

$$\mathcal{H}[\sigma(\omega, t, t_w)] = \Re[\mathcal{H}[\epsilon_a(\omega, t) G^*(\omega, t, t_w)]]. \quad (\text{E8})$$

Assuming the spectra of $G^*(\omega, t, t_w)$ for t and spectra of the input shear strain, ω , satisfy the Bedrosian's theorem,

$$\begin{aligned} \mathcal{H}[\sigma(\omega, t, t_w)] &= \Re[\mathcal{H}[\epsilon_a(\omega, t) G^*(\omega, t, t_w)]] \\ &= \Re[-i\epsilon_a(\omega, t) G^*(\omega, t, t_w)] \\ &= \Im[\epsilon_a(\omega, t) G^*(\omega, t, t_w)]. \end{aligned} \quad (\text{E9})$$

Thus, from the definition of analytic signal [Eq. (E3)] with Eqs. (E6) and (E9), the analytic signal of $\sigma(\omega, t, t_w)$ is written as

$$\sigma_a(\omega, t, t_w) = \epsilon_a(\omega, t) G^*(\omega, t, t_w). \quad (\text{E10})$$

Therefore the definition of the instantaneous complex modulus, Eq. (11), gives

$$G(\omega, t, t_w) \equiv \frac{\sigma_a(\omega, t, t_w)}{\epsilon_a(\omega, t)} = G^*(\omega, t, t_w). \quad (\text{E11})$$

This shows that, under the Bedrosian's theorem, the instantaneous complex modulus and the viscoelastic spectra are identical.

It may be instructive to consider the simple Maxwell fluid. Because the Hilbert transform is a linear transform, we can write the constitutive equation of simple Maxwell fluid using analytic signal,

$$\dot{\epsilon}_a(t) = \frac{\sigma_a(t)}{\eta_0} + \frac{\dot{\sigma}_a(t)}{G_0}. \quad (\text{E12})$$

Let us consider the input stress $\sigma(\omega, t) = \sigma_0 \cos(\omega t)$. The analytic signal of $\sigma(\omega, t)$ is $\sigma_a(\omega, t) = \sigma_0 e^{i\omega t}$. The explicit integration of right-hand side, setting integration constant 0, to obtain $\epsilon_a(\omega, t)$ leads to $\epsilon_a(\omega, t) = \sigma_0 e^{i\omega t} (1/G_0 - i/(\eta_0\omega))$. Therefore $G(\omega, t) = \sigma_a(\omega, t)/\epsilon_a(\omega, t) = 1/(1/G_0 - i/(\eta_0\omega))$, which is the complex modulus of Maxwell fluid which does not have time dependence. Therefore, Eq. (11) recovers the definition of conventional complex modulus.

APPENDIX F: AGING FLUCTUATION-DISSIPATION THEOREM FOR MAXWELL GLASS

We first obtain the strain-stress response function, $\chi(t, t')$, for the constitutive equation, Eq. (4):

$$\begin{aligned} \epsilon(t) &= \int_0^t \Theta(t-t') \left(\frac{P_u(t')}{\eta_0} + \frac{1}{G_0} \frac{d}{dt'} \right) \sigma(t') dt' \\ &= \int_0^t \left(\Theta(t-t') \frac{P_u(t')}{\eta_0} + \frac{2\delta(t-t')}{G_0} \right) \sigma(t') dt', \quad (\text{F1}) \end{aligned}$$

where $\Theta(t)$ is the Heaviside step function. The factor 2 in front of the delta function is to account for the boundary. Therefore the response function is given as

$$\chi(t, t') = \Theta(t-t') \frac{P_u(t')}{\eta_0} + \frac{2\delta(t-t')}{G_0}. \quad (\text{F2})$$

On the other hand, using Eq. (17) and the constant $4k_B T/G_0$, we compute

$$\begin{aligned} &\Theta(t-t') \frac{d}{dt'} \langle \Delta x^2(t') \rangle \\ &= \Theta(t-t') \left(2D_0 P_u(t') + \frac{d}{dt'} \frac{4k_B T}{G_0} \right) \\ &= 2k_B T \left(\Theta(t-t') \frac{P_u(t')}{\eta_0} + \frac{2\delta(t-t')}{G_0} \right), \quad (\text{F3}) \end{aligned}$$

where we used integration by parts from the second line to the third line and the Einstein relation $D_0 \eta_0 = k_B T$ [46]. Therefore we obtain the fluctuation-response relation, Eq. (21).

The response function $\chi(t, t')$ is related to the dynamic modulus $G(t, t')$ by inverse, thus uniquely determined. To see this we notice that the shear strain $\epsilon(t)$ is written using

Eqs. (A1) and (A4) as

$$\begin{aligned} \epsilon(t) &= \int_0^t dt' \chi(t, t') \int_0^{t'} dt'' G(t', t'') \epsilon(t'') \\ &= \int_0^t dt'' \epsilon(t'') \int_{t''}^t dt' \chi(t, t') G(t', t''). \quad (\text{F4}) \end{aligned}$$

By direct calculation using Eqs. (F2) and (A3) and using that the general form of $K(t, t')$ in our model [Eq. (6)] has exponential form, we obtain

$$\int_{t''}^t dt' \chi(t, t') G(t', t'') = 2\delta(t-t''), \quad (\text{F5})$$

leading to the consistent expression for Eq. (F4). Note that the factor 2 accounts for the integration of the delta function at the boundary. Equation (F5) shows that $\chi(t, t')$ and $G(t, t')$ are related by inverse and uniquely determined.

APPENDIX G: NUMERICAL PROCEDURE TO SOLVE THE TRAP MODEL FOR THE PROTEIN CONDENSATES

To numerically solve the dynamical equations describing trap dynamics Eq. (1) we discretize the time and energy. In particular, we use the time step $\Delta t = 0.01/\Gamma_0$ and the energy step $\Delta E/(k_B T) = 0.02$. We choose units of time and energy by setting $1/\Gamma_0 = 1$ and $k_B T = 1$. For the numerical computation it is necessary to introduce the cutoff for the energy. We set the maximum energy to be $E_M = 100$ in units of $k_B T$. We evaluate integrals numerically as a sum of the discretised integrand values multiplied by ΔE . We use the Euler method for the integration over time.

APPENDIX H: NUMERICAL PROCEDURES TO COMPUTE INSTANTANEOUS COMPLEX MODULUS

To compute the instantaneous complex modulus $G(\omega, t, t_w)$, we employed the analytic signal approach to obtain the instantaneous amplitude and phase of the input and output signals. Specifically, we utilized the Python package “scipy.signal.hilbert” [47] to extract the instantaneous amplitude and phase for the input shear strain and output shear stress, as illustrated in Fig. 6. This method allowed us to accurately capture the time-varying behavior of the signals and determine the complex modulus at any given time and frequency.

The computation of the instantaneous complex modulus $G(\omega, t, t_w)$, as defined in Eq. (11), requires the input shear strain $\epsilon(\omega, t)$ to span from $t = -\infty$ to $t = \infty$. Practically, when implementing the numerical computation of instantaneous complex modulus, we extrapolate the input shear strain used in the rheology experiment. Here we extended the imposed sinusoidal shear strain starting $t = t_w$ and ending $t = t_f$: $\epsilon(\omega, t) \Theta(t-t_w) \Theta(t_f-t)$, to the signal from $t = t_w - \tau$ to $t = t_f + \tau$, where $\tau = t_f - t_w$ is the duration of the shear strain. For the output shear stress, we inserted 0 from $t = t_w - \tau$ to $t = t_w$ and from $t = t_f$ to $t = t_f + \tau$, to adjust the length of the input and output signals. After the extension of the input shear strain and output shear stress we computed Hilbert transform and then extracted back the original, experimentally relevant, part of the signal defined from $t = t_w$

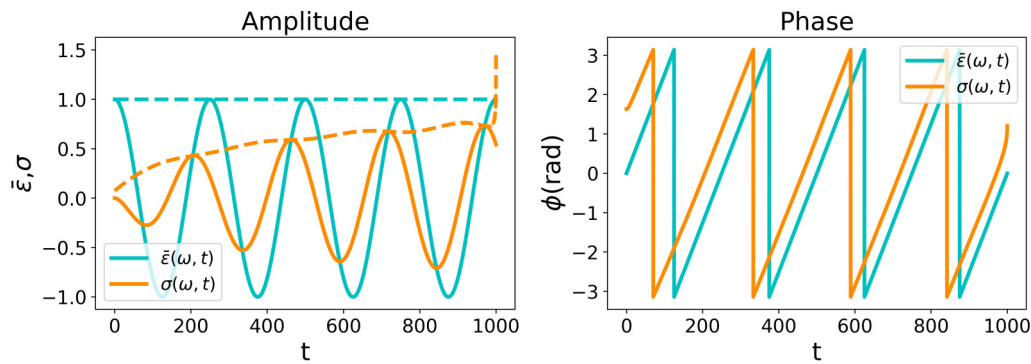


FIG. 6. An example of the instantaneous amplitude and phase extraction using analytic signal. Left: Amplitude extraction from the data using analytic signal. The solid line in cyan is the input strain $\bar{\epsilon}(\omega, t)$, and the solid orange line is the output stress $\sigma(\omega, t)$. Dashed curves are the instantaneous amplitude of $\bar{\epsilon}(\omega, t)$ and $\sigma(\omega, t)$, computed using analytic signal. Right: Instantaneous phase for $\epsilon(\omega, t)$ (cyan) and $\sigma(\omega, t)$ (orange), computed using analytic signal.

to $t = t_f$. We computed the instantaneous complex modulus using the obtained analytic signal for the input shear strain and output shear stress.

The Hilbert transform, computed using Fourier transform as shown in Eq. (E2), may produce unwanted oscillations, known as the Gibbs phenomenon, due to the finite discontinuous signal (as illustrated in Fig. 6). To obtain accurate results,

we truncated the two edges of the complex modulus, i.e., the initial and final times where the artifact is most prominent. Additionally, we convolved the resulting $G(\omega, t, t_w)$ with a box kernel whose length was identical to the wavelength of the input shear strain to mitigate the oscillations caused by the Gibbs phenomenon. This step helped to improve the accuracy of our results, shown in Fig. 3.

- [1] S. F. Banani, H. O. Lee, A. A. Hyman, and M. K. Rosen, Biomolecular condensates: Organizers of cellular biochemistry, *Nat. Rev. Mol. Cell Biol.* **18**, 285 (2017).
- [2] C. P. Brangwynne, C. R. Eckmann, D. S. Courson, A. Rybarska, C. Hoegge, J. Gharakhani, F. Jülicher, and A. A. Hyman, Germline P granules are liquid droplets that localize by controlled dissolution/condensation, *Science* **324**, 1729 (2009).
- [3] A. A. Hyman, C. A. Weber, and F. Jülicher, Liquid-liquid phase separation in biology, *Annu. Rev. Cell Dev. Biol.* **30**, 39 (2014).
- [4] A. Ghosh, D. Kota, and H.-X. Zhou, Shear relaxation governs fusion dynamics of biomolecular condensates, *Nat. Commun.* **12**, 5995 (2021).
- [5] L. Jawerth, E. Fischer-Friedrich, S. Saha, J. Wang, T. Franzmann, X. Zhang, J. Sachweh, M. Ruer, M. Ijavi, S. Saha *et al.*, Protein condensates as aging Maxwell fluids, *Science* **370**, 1317 (2020).
- [6] J. A. Riback, J. M. Eeftens, D. S. Lee, S. A. Quinodoz, L. Beckers, L. A. Becker, and C. P. Brangwynne, Viscoelastic RNA entanglement and advective flow underlies nucleolar form and function, *Biophys. J.* **121**, 473a (2022).
- [7] T. M. Franzmann, M. Jahnel, A. Pozniakovskiy, J. Mahamid, A. S. Holehouse, E. Nüske, D. Richter, W. Baumeister, S. W. Grill, R. V. Pappu *et al.*, Phase separation of a yeast prion protein promotes cellular fitness, *Science* **359**, eaao5654 (2018).
- [8] A. Patel, H. O. Lee, L. Jawerth, S. Maharana, M. Jahnel, M. Y. Hein, S. Stoykov, J. Mahamid, S. Saha, T. M. Franzmann *et al.*, A liquid-to-solid phase transition of the ALS protein FUS accelerated by disease mutation, *Cell* **162**, 1066 (2015).
- [9] Y. Shin and C. P. Brangwynne, Liquid phase condensation in cell physiology and disease, *Science* **357**, eaaf4382 (2017).
- [10] L. Berthier and G. Biroli, Theoretical perspective on the glass transition and amorphous materials, *Rev. Mod. Phys.* **83**, 587 (2011).
- [11] T. R. Kirkpatrick and D. Thirumalai, *Colloquium*: Random first order transition theory concepts in biology and physics, *Rev. Mod. Phys.* **87**, 183 (2015).
- [12] I. Alshareedah, M. M. Moosa, M. Pham, D. A. Potoyan, and P. R. Banerjee, Programmable viscoelasticity in protein-RNA condensates with disordered sticker-spacer polypeptides, *Nat. Commun.* **12**, 6620 (2021).
- [13] H.-X. Zhou, Shape recovery of deformed biomolecular droplets: Dependence on condensate viscoelasticity, *J. Chem. Phys.* **155**, 145102 (2021).
- [14] H.-X. Zhou, Viscoelasticity of biomolecular condensates conforms to the Jeffreys model, *J. Chem. Phys.* **154**, 041103 (2021).
- [15] L. Meng and J. Lin, Indissoluble biomolecular condensates via elasticity, *Phys. Rev. Res.* **5**, L012024 (2023).
- [16] Y. Shen, A. Chen, W. Wang, Y. Shen, F. S. Ruggeri, S. Aime, Z. Wang, S. Qamar, J. R. Espinosa, A. Garaizar, P. St George-Hyslop, R. Collepardo-Guevara, D. A. Weitz, D. Vigolo, and T. P. J. Knowles, Solid/liquid coexistence during aging of FUS condensates, *bioRxiv* (2022).
- [17] D. T. N. Chen, Q. Wen, P. A. Janmey, J. C. Crocker, and A. G. Yodh, Rheology of soft materials, *Annu. Rev. Condens. Matter Phys.* **1**, 301 (2010).
- [18] D. Doraiswamy, The origins of rheology: A short historical excursion, *Rheology Bull.* **71**, 1 (2002).
- [19] L. C. E. Struik, *Physical Aging in Amorphous Polymers and Other Materials*, Vol. 106 (Elsevier, Amsterdam, 1978).

- [20] S. Jabbari-Farouji, D. Mizuno, M. Atakhorrami, F. C. MacKintosh, C. F. Schmidt, E. Eiser, G. H. Wegdam, and D. Bonn, Fluctuation-Dissipation Theorem in an Aging Colloidal Glass, *Phys. Rev. Lett.* **98**, 108302 (2007).
- [21] S. M. Fielding, P. Sollich, and M. E. Cates, Aging and rheology in soft materials, *J. Rheology* **44**, 323 (2000).
- [22] P. Sollich, Rheological constitutive equation for a model of soft glassy materials, *Phys. Rev. E* **58**, 738 (1998).
- [23] P. Sollich, F. Lequeux, P. Hébraud, and M. E. Cates, Rheology of Soft Glassy Materials, *Phys. Rev. Lett.* **78**, 2020 (1997).
- [24] J.-P. Bouchaud, Weak ergodicity breaking and aging in disordered systems, *J. Phys. I (France)* **2**, 1705 (1992).
- [25] C. Monthus and J.-P. Bouchaud, Models of traps and glass phenomenology, *J. Phys. A* **29**, 3847 (1996).
- [26] J. Lin, Modeling the aging of protein condensates, *Phys. Rev. Res.* **4**, L022012 (2022).
- [27] J. C. Phillips, Stretched exponential relaxation in molecular and electronic glasses, *Rep. Prog. Phys.* **59**, 1133 (1996).
- [28] J. Wuttke, W. Petry, and S. Pouget, Structural relaxation in viscous glycerol: Coherent neutron scattering, *J. Chem. Phys.* **105**, 5177 (1996).
- [29] E. M. Furst and T. M. Squires, *Microrheology* (Oxford University Press, Oxford, 2017).
- [30] R. Kubo, M. Toda, and N. Hashitsume, *Statistical Physics II: Nonequilibrium Statistical Mechanics* (Springer Science & Business Media, New York, 2012), Vol. 31.
- [31] T. G. Mason, Estimating the viscoelastic moduli of complex fluids using the generalized Stokes-Einstein equation, *Rheol. Acta* **39**, 371 (2000).
- [32] P. J. Flory, Thermodynamic relations for high elastic materials, *Trans. Faraday Soc.* **57**, 829 (1961).
- [33] H. S. Fricker, The effects on rubber elasticity of the addition and scission of cross-links under strain, *Proc. R. Soc. London A* **335**, 267 (1973).
- [34] F. Tanaka and S. F. Edwards, Viscoelastic properties of physically crosslinked networks. 1. Transient network theory, *Macromolecules* **25**, 1516 (1992).
- [35] F. Tanaka and S. F. Edwards, Viscoelastic properties of physically crosslinked networks: Part 2. Dynamic mechanical moduli, *J. Non-Newtonian Fluid Mech.* **43**, 273 (1992).
- [36] P. Hébraud and F. Lequeux, Mode-Coupling Theory for the Pasty Rheology of Soft Glassy Materials, *Phys. Rev. Lett.* **81**, 2934 (1998).
- [37] A. Nicolas, E. E. Ferrero, K. Martens, and J.-L. Barrat, Deformation and flow of amorphous solids: Insights from elastoplastic models, *Rev. Mod. Phys.* **90**, 045006 (2018).
- [38] P. Sollich, J. Olivier, and D. Bresch, Aging and linear response in the Hébraud-Lequeux model for amorphous rheology, *J. Phys. A* **50**, 165002 (2017).
- [39] L. Berthier, L. F. Cugliandolo, and J. L. Iguain, Glassy systems under time-dependent driving forces: Application to slow granular rheology, *Phys. Rev. E* **63**, 051302 (2001).
- [40] L. F. Cugliandolo, The effective temperature, *J. Phys. A* **44**, 483001 (2011).
- [41] L. F. Cugliandolo, J. Kurchan, and L. Peliti, Energy flow, partial equilibration, and effective temperatures in systems with slow dynamics, *Phys. Rev. E* **55**, 3898 (1997).
- [42] M. Abramowitz and I. A. Stegun, *Handbook of Mathematical Functions with Formulas, Graphs, and Mathematical Tables* (Dover, New York, 1964), Vol. 55.
- [43] F. W. King, *Hilbert Transforms Vol. 1*, Vol. 124 of Encyclopedia of Mathematics and Its Applications (Cambridge University Press, Cambridge, 2009).
- [44] F. W. King, *Hilbert Transforms: Volume 2* (Cambridge University Press, Cambridge, 2009).
- [45] E. Bedrosian, A product theorem for Hilbert transforms, Technical report (Rand Corporation, Santa Monica, CA, 1962).
- [46] R. Zwanzig, *Nonequilibrium Statistical Mechanics* (Oxford University Press, Oxford, 2001).
- [47] P. Virtanen, R. Gommers, T. E. Oliphant, M. Haberland, T. Reddy, D. Cournapeau, E. Burovski, P. Peterson, W. Weckesser, J. Bright, S. J. van der Walt, M. Brett, J. Wilson, K. J. Millman, N. Mayorov, A. R. J. Nelson, E. Jones, R. Kern, E. Larson, C. J. Carey, Í. Polat *et al.*, SciPy 1.0 Contributors, SciPy 1.0: Fundamental Algorithms for Scientific Computing in Python, *Nat. Methods* **17**, 261 (2020).